Nuclear Engineering and Technology 54 (2022) 4005–4012

Contents lists available at ScienceDirect

Nuclear Engineering and Technology

journal homepage: www.elsevier.com/locate/net

Original Article

Evaluation on the buffer temperature by thermal conductivity of gap-filling material in a high-level radioactive waste repository

Seok Yoon [a], Min-Jun Kim [b], Seeun Chang [c], Gi-Jun Lee [a, *]

[a] Disposal Safety Evaluation Research Division, Korea Atomic Energy Research Institute (KAERI), Daejeon, 34057, South Korea
[b] Geology Division, Korea Institute of Geoscience and Mineral Resources (KIGAM), Daejeon, 34132, South Korea
[c] Radioactive Waste Disposal Team, Korea Atomic Energy Research Institute (KAERI), Daejeon, 34057, South Korea

ARTICLE INFO

Article history:
Received 6 February 2022
Received in revised form
31 May 2022
Accepted 7 June 2022
Available online 12 June 2022

Keywords:
Engineered barrier system
Gap spacing
Gap-filling material
Granular bentonite

ABSTRACT

As high-level radioactive waste (HLW) generated from nuclear power plants is harmful to the human body, it must be safely disposed of by an engineered barrier system consisting of disposal canisters and buffer and backfill materials. A gap exists between the canister and buffer material in a HLW repository and between the buffer material and natural rock—this gap may reduce the water-blocking ability and heat transfer efficiency of the engineered barrier materials. Herein, the basic characteristics and thermal properties of granular bentonite, a candidate gap-filling material, were investigated, and their effects on the temperature change of the buffer material were analyzed numerically. Heat transfer by air conduction and convection in the gap were considered simultaneously. Moreover, by applying the Korean reference disposal system, changes in the properties of the buffer material were derived, and the basic design of the engineered barrier system was presented according to the gap filling material (GFM). The findings showed that a GFM with high initial thermal conductivity must be filled in the space between the buffer material and rock. Moreover, the target dry density of the buffer material varied according to the initial wet density, specific gravity, and water content values of the GFM.

1. Introduction

Spent nuclear fuel (SNF) is a high-level radioactive waste (HLW) generated in nuclear power plants, and it is very dangerous to the human body owing to its intense radiation emissions. Therefore, as this HLW must be completely isolated from human life zone, it must be safely disposed of in bedrock at a depth of several hundred meters by a multibarrier system composed of natural and engineered barriers [1–3]. Natural barriers refer to rock and geological environments that exist in a natural state around the HLW repository, and engineered barriers artificially developed by humans, which consist of disposal canisters, and buffer and backfill materials. An HLW repository consists of several disposal tunnels and their interconnecting tunnels. A vertical deposition hole is excavated at the bottom of the disposal tunnels [4,5]. Subsequently, the SNF is sealed in the disposal canister, the disposal canister is left in the deposition hole, the empty space between the disposal canister and rock is filled with buffer materials, and the disposal tunnels are filled with backfill materials to close them completely.

The engineered barrier delays the penetration of groundwater existing in the rock around the HLW repository and plays a role in preventing the leakage of radionuclides contained in HLW to the outer parts of the repository [6]. In engineered barrier systems, compacted bentonite made of bentonite powders, is known to be the most suitable buffer material [7–10]. In Korea, studies on the effects of thermal conductivity [3,11,12], water suction analysis with saturation condition [3], and hydraulic conductivity with temperature [13] and unsaturated state [14], and safety analysis [15] as well as basic properties such as swelling index and components [16] on a buffer material for bentonite produced in Gyeongju, have been conducted. When the disposal canister is placed in the deposition hole of the HLW repository and buffer materials are installed, gaps are inevitably formed between the disposal canister and buffer materials, and between the buffer materials and the rock, as shown in Fig. 1. This is attributed to the fact that during the installation of buffer or backfill materials, a specific volume in space must be provided for the convenience of work, and the fact that the rock surfaces of the excavated deposition holes are uneven [17]. However, if these gaps exist after the HLW repository is closed, the

* Corresponding author.
E-mail address: gijunlee@kaeri.re.kr (G.-J. Lee).

https://doi.org/10.1016/j.net.2022.06.008

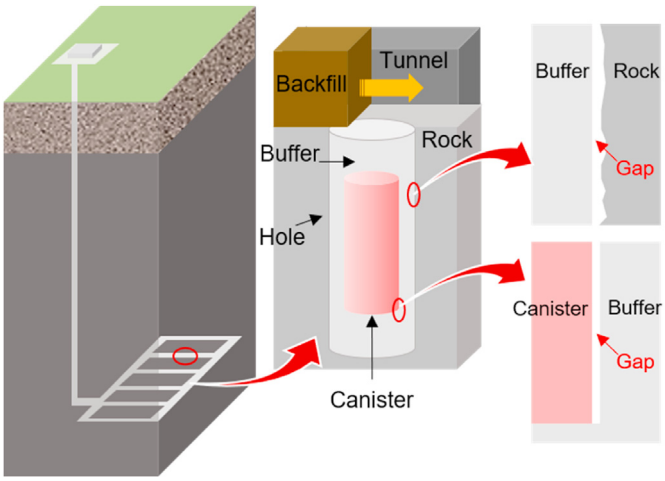

Fig. 1. Gap space in the engineered barrier system.

water-blocking ability and heat transfer efficiency of the engineered barrier materials will decrease. Thus, the gaps must be filled with specific materials [4].

Therefore, it is necessary to study the gap sizes and gap filling materials (GFMs) in deposition holes. Relevant research is mainly being conducted in Sweden and Finland. Sweden and Finland allow a 10-mm gap between the disposal canister and the buffer material, and a 50-mm gap between the buffer material and the rock on the inner wall of the deposition hole. Additionally, they do not fill the gap between the disposal canister and buffer material; bentonite pellets between the buffer material and inner wall of the deposition hole and granular bentonite are applied as GFMs [4,18]. In Canada, an experiment was conducted to fill the gap between the buffer material and rock with bentonite pellets and granular bentonite [19]. Lee et al. [20] showed that filling the gap between the disposal canister and the buffer material increased the peak temperature of the buffer material. In general, the gap between the disposal canister and buffer material was not filled.

However, compared with buffer materials and disposal canisters, research on GFMs is incomplete, and applicable research on GFMs to real fields except for the above research conducted in Sweden, Finland [4,18], and Canada [19] is limited. In addition, data on the properties of candidate materials for GFMs are very scarce [21]. Consequently, it is necessary to analyze the effect of the properties of GFMs on the target properties of the buffer materials. Therefore, in this study, a basic physical and thermal property database for granular bentonite was established, and the temperature change of the buffer material was analyzed based on numerical analysis by reflecting the thermal properties of granular bentonite considering the gap between the canister and buffer material. In addition, an attempt was made to present a design proposal for a GFM according to the Korean reference disposal system. Therefore, this study, for the first time, suggests guidelines for the design criteria for GFMs, such as injection volume and swelling ability of granular bentonite, considering the basic properties of the bentonite that satisfy the conditions of Korean reference disposal system.

2. Materials and methods

2.1. Basic properties and chemical compositions

Granular bentonite was manufactured with a pellet production apparatus. If bentonite powder is poured into the apparatus, it is squeezed out through the gap between the upper and lower two rollers. In the case of bentonite powder, the swelling pressure is very low due to the low density. Therefore, to fill the gaps well, granular bentonite with a size of 1–2 mm having a higher dry density than that of the bentonite powder was rolled into a very small gap as well. In this study, a basic property and chemical composition evaluation of granular bentonite produced by Clariant Korea Co., Ltd., was conducted. Table 1 lists the basic properties of granular bentonite and KJ-II bentonite powders, which were Ca-type bentonite produced in Gyeongju, Korea [16]. Table 2 lists X-ray diffraction analysis outcomes, and Table 3 lists the X-ray fluorescence analysis results.

Granular bentonite was also classified as high-density clay (CH) (similar to the classification of KJ-II as bentonite clay), and the montmorillonite content was also derived similar to that of KJ-II. However, in the case of granular bentonite, which is a Na-type bentonite, the swelling index was derived to be more than three times larger than that of KJ-II. Since GFMs must fill the gaps well, a Na-type bentonite with better swelling ability than that of KJ-II [22] was used for the GFM material, which is the granular type for this study. The organic carbon and sulfide contents of the buffer material should be less than 0.5% [4]. It is known that organic carbon below 0.5% does not affect considerably the physical and mechanical properties of the buffer material [23]. Organic carbon and sulfur contents used in this test were derived using a Carbon/Sulfur Analyzer (CS-800, ELTRA, City, State, Country). Each sample (about 30 mg) was burnt at a high temperature of approximately 2000 °C to simultaneously analyze the total carbon and sulfur contents. The analysis method based on high temperature combustion rapidly oxidized almost all carbon contained in the sample. Thus, it is considered the most reliable method among carbon analysis methods [24]. The hydrochloric acid (HCl) was used to make the sample acidified, and analysis was performed following the removal of inorganic carbon from the sample [25]. No pretreatment was applied for sulfur measurement. As a result of the analysis, the organic carbon and sulfur content of granular bentonite and KJ-II powder bentonite were both measured to be less than 0.5%, respectively, it means that measured organic carbon and sulfur contents did not affect the physical and mechanical properties of the buffer material.

2.2. Thermal properties

To analyze the effect of the thermal properties of the GFM on the temperature change of the buffer material, the thermal properties such as thermal conductivity and specific heat capacity of granular bentonites should be measured. As granular bentonite is a porous material that will be installed in a free-fall form in the gap between the rock and buffer material of the deposition hole, thermal conductivity and specific heat were measured in the initial granular and powder states, but not in the compressed state. First, the thermal conductivity of granular bentonite was measured using a single KD2-pro probe, an abnormal probe device. The single probe method is a method used to measure the thermal conductivity from the increasing temperature trend of the metal wire as a function of time, while concurrently applying a current to the very thin metal wire based on the infinite linear heat source theory [26,27]. Additionally, the specific heat capacity was measured with the use of a dual-probe method that calculated the volume specific heat using the time and the temperature in the case in which the heat applied to one probe then reached the other based on the infinite linear heat source theory [28]. Fig. 2 shows the process of measuring the thermal properties of granular bentonite with the use of a probe. In particular, a fixture was used to fix the probe in the sample. Table 4 shows the thermal conductivity and specific heat capacity values of

Table 1
Basic properties of bentonite granules and KJ-II bentonite powders.

	Specific gravity	Liquid limit (%)	Plastic limit (%)	USCS	Swelling index (ml/2g)	Initial water content (%)	Specific area (m^2/g)	Passing 2um (%)	Organic Carbon content (%)	S content (%)
KJ-II	2.71	146.7	28.4	CH	6.5	11–12	61.5	48.4	0.25	0.3
Granular bentonite	2.7	130.6	33	CH	20.5	11–12	12.61	80.9	0.13	0.009

Table 2
Quantitative XRD analysis of bentonite granules and KJ-II bentonite powders.

Mineral composition (%)	Montmorillonite	Albite	Quarts	Cristobalite	Calcite	Heulandite	Dolomite	Biotite
KJ-II	61.9	20.9	5.3	4.1	7.4	3.0	–	–
Granular bentonite	60.3	9.9	–	20.5 (Cristobalite/Opal)	2.7	5 (Heulandite/Clinoptilolite)	1.8	Trace

Table 3
Chemical composition of bentonite granules and KJ-II bentonite powders.

Chemical constituent (%)	SiO_2	Al_2O_3	Fe_2O_3	CaO	MgO	K_2O	Na_2O	TiO	MnO	P_2O_5	Ig. Loss
KJ-II	58.81	15.17	5.28	5.72	2.70	1.27	1.06	0.67	0.13	–	–
Granular bentonite	65.91	13.37	0.94	2.55	2.76	1.17	4.63	0.15	0.07	0.02	8.19

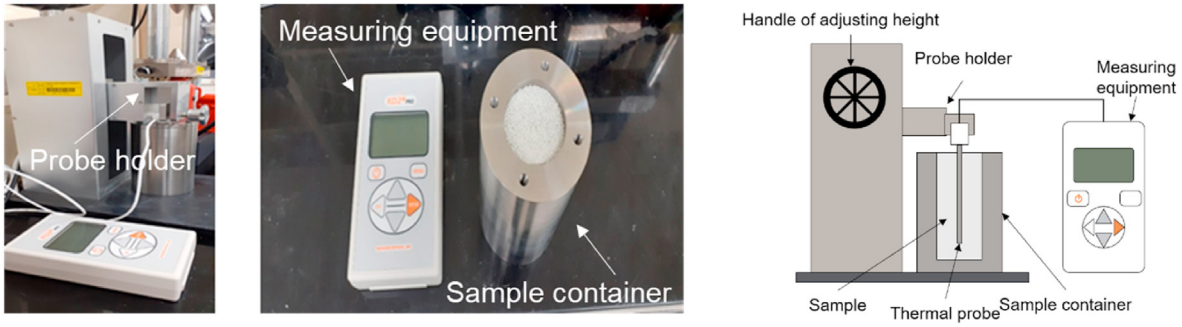

Fig. 2. Test procedure: (a) Digital images of test process, (b) schematic diagram of the test procedure.

Table 4
Thermal properties of bentonite granules and KJ-II bentonite powders.

	Dry density (g/cm^3)	Thermal conductivity (W/(m·K))	Specific heat (kJ/(kg·K))
KJ-II	0.98	0.092–0.099	0.873–0.877
	0.89	0.085	0.919
Granular bentonite			1.275

KJ-II and granular bentonite for the wet density of ~1 g/cm^3, which could be formed by falling samples. The thermal conductivity of granular bentonite was larger than that of KJ-II. For this reason, it is inferred that granular bentonite contained cristobalite mineral with a high thermal conductivity (which was five times more than that of KJ-II), and the initial particle size of granular bentonite was in the range of 1–2 mm, which is several tens of times larger than that of KJ-II bentonite powder.

3. Numerical analysis

In this study, numerical analysis was performed to evaluate the effect of the GFM properties on the temperature changes of the buffer materials in the engineered barrier. For numerical analysis, the commercial program COMSOL Multiphysics (version 5.5, manufacturer, City, State, Country) based on continuum analysis and the finite element method was used. COMSOL Multiphysics is capable of solving the governing equations according to various analysis modules, using the most suitable configuration model, and fully coupled analysis between each module. If necessary, the user can directly compose equations [29]. In particular, the reliability of the use of this program has been demonstrated by several research studies which performed coupled analysis on HLW repositories [5,14,30]. In this study, the heat transfer and laminar flow modules of the program were used to evaluate the peak temperature of the buffer material.

3.1. Constitutive equations

In the analysis of the temperature changes of the buffer material owing to the heat generated from the SNF, heat conduction was considered in the components of the entire disposal system. In particular, in the gap between the disposal canister and the buffer material, heat transfer may occur owing to air conduction and convection. Thus, in this study, the temperature change of the buffer material was derived by considering the heat transfer attributed to air conduction and convection in the gap at the same time. The heat transfer governing equation of the heat transfer module considered in the disposal system is as follows.

$$\rho C_p \frac{\partial T}{\partial t} + \rho C_p u \cdot \nabla T + \nabla \cdot (\lambda \nabla T) = Q \tag{1}$$

where T is the temperature of the medium (K), t is the time (s), ρ is the density of the medium (kg/m^3), C_p is the specific heat of the medium (J/(kg·K)), u is the velocity of the medium (m/s), λ is the thermal conductivity (W/(m·K)), and Q is the general heat source (W/m^3). Given that there was no medium velocity in the disposal canister, and no buffer material, backfill material, and rock (with the exception of the gap), only heat conduction (excluding the convection term) was considered in Eq. (1). In the gap of the engineered barrier, forced convection was not considered because there were no artificial boundaries and flow conditions for air. Thus, only natural convection, which was caused by temperature differences and gravity, was considered. Laminar flow and turbulence can occur in natural convection, and the flow pattern that determines this depends on the Grashof number that represents the ratio of the buoyant force to the viscous force acting on the fluid. In this study, only laminar flow was considered because the Grashof number for air flow in the gap was smaller than the standard value for transition to turbulence equal to 10^9 [31]. Therefore, the flow module in laminar flow conditions was used to consider convection, which corresponds to the heat transferred according to the flow of air in the gap. The flow in a single gas can be considered by the Navier–Stokes law, and the governing equation of the laminar low module is as follows:

$$\rho \frac{\partial u}{\partial t} + \rho(u \cdot \nabla)u = \nabla \cdot (-pI + \tau) + \rho g \tag{2}$$

where p is the pressure (Pa), τ is the viscous stress tensor (Pa), and g is the acceleration of gravity (m/s^2). With respect to the velocity of the medium, which is commonly formulated according to Eqs. (1) and (2), air properties in the gap are combined, and heat transfer during air convection is reflected in the analysis. In addition, in this study, the behavior of incompressible fluids was considered, and the Boussinesq approximation method was applied to the analysis [17].

3.2. Methods and processes

In reality, heat is dissipated inside the canister, continuously sent to the interface of the canister, and transferred to the buffer through the air layer, so it is important to implement this process [32]. Thus, in this numerical analysis, temperature was continuously generated on the surface of the canister based on the heat generation rate by HLW, and the amount of heat transferred to the buffer material through the air from the interface between the canister and air layer was studied. In this study, the Improved Korea Atomic Energy Research Institute reference disposal system (KRS$^+$), which was proposed to dispose of PWR SNF generated in Korea, was considered as an analysis model [15]. Based on the concept of engineered multibarriers, a two-dimensional (2D), axially symmetric, finite element model was established. The installation depth was assumed to be 500 m, and the disposal tunnel, disposal canister, backfill material, buffer material, gap, and near-field rock, which are components of the disposal system, were all considered in the analysis model. The gap in the engineered barrier occurred in two places: the interface between the disposal canister and the buffer material and the interface between the buffer material and the near-field rock. The analysis model is shown in Fig. 3.

High-level radioactive SNF is stored in a disposal canister after a temporary storage period of approximately 50 years in a temporary storage tank [15]. The decay heat generated in the disposal canister after the temporary storage period has a tendency to gradually decrease over time (owing to the material's half-life) and can be expressed according to Eq. (3) [15].

$$Y = y_0 + A_1 \times \exp\left(-\frac{t - x_0}{t_1}\right) + A_2 \times \exp\left(-\frac{t - x_0}{t_2}\right) + A_3 \times \exp\left(-\frac{t - x_0}{t_3}\right) \tag{3}$$

where Y is the amount of decay heat emitted from the disposal canister (W), and t is the analysis period (year). x_0, y_0, A_1, A_2, A_3, t_1, t_2, and t_3 are the constants from Lee et al. [15]. In the numerical analysis model, decay heat as a function of time was set by substituting Eq. (3) for the heat source generated in the disposal canister.

In addition, in the analysis, the standard properties of the KRS$^+$ were used for the thermal properties of each component of the disposal system, as shown in Table 5. For the thermal properties of granular bentonites applied as GFMs, the values derived from Section 2.2 were used, and for the properties of other elements, the values from Lee et al. [15] and Kim et al. [33] were used. Analysis was performed by setting the analysis period to 20 years to confirm the peak temperature according to the operation of the disposal system. In Eq. (3), as the heat generated from the SNF continuously decreases with time, it can be considered as a sufficient analysis period to confirm the peak temperature. To consider the accuracy and efficiency of the analysis simultaneously, the mesh was formed densely in the gap near the heat source and in the vicinity of the buffer material, and the rock part far away from the heat source was formed loosely. The generated mesh consisted of 2D elements in the shape of triangles, and a total number of 71,606 elements were set. Regarding the boundary conditions applied for numerical analysis, the left side was set as a 2D axisymmetric condition, and

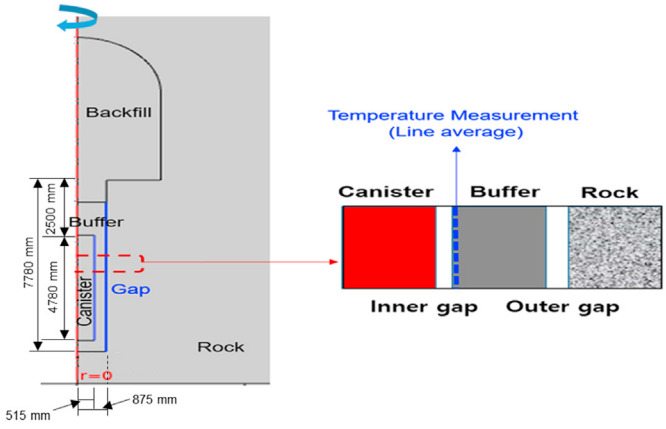

Fig. 3. Geometry of the gap spaces in the numerical model.

Table 5
Input properties used in the numerical analysis.

		Thermal conductivity (W/(m·k))	Density (kg/m^3)	Specific heat capacity (J/(kg·K))
Canister[a]	Copper shell	386	8900	383
	Cast insert	52	7200	504
Backfill[a]		0.8	1970	1380
Buffer[b]		1	1970	1380
Gap (Air)		0.025	1.293	1.01
Gap (granular bentonite)		0.158	1000	1275
Rock[1]		2	2270	1190

Note.
[a] Input parameters of the canister, the backfill, and the rock were from Ref. [16].
[b] Input parameter of the buffer was from Ref. [15].

the other side was set as an adiabatic condition. As the initial condition, the surface temperature was set to 10 °C, and a geothermal gradient (3 °C/100 m) in which the temperature increased as the depth increased was applied in the overall analysis model. An adiabatic condition was set in common at the upper and lower boundaries of the gap as the heat transfer boundary condition for natural convection analysis within the gap. Based on the buffer material, there are interfaces between the canister and buffer material and between the buffer material and the rock. Thus, the average temperature of the disposal canister was set at the left boundary of the gap between the disposal canister and buffer material, and the average temperature of the buffer material was set at the right boundary. The average temperature of the buffer material was set at the left boundary of the gap between the buffer material and the rock, and the average temperature of the rock was set at the right boundary. In addition, in the laminar flow analysis, flow due to gravity and density differences within the gap was considered, and a condition in which no flow occurred at all interfaces of the gap was set. The main monitoring point is the interface between buffer material and canister shown in Fig. 3. In other words, it is right boundary of the gap between the canister and buffer material.

4. Results and discussions

4.1. GFM application results

Given that heat transfer owing to conduction and convection by air can occur in the gap between the disposal canister and the buffer material, in this study, the peak temperature of the buffer material was derived by considering the heat transfer induced by the conduction and convection of air in the gap simultaneously. First, to analyze the importance of the gap, the peak temperature of the buffer material was calculated with and without the gap (Fig. 4). The space between the disposal canister and the buffer material was set

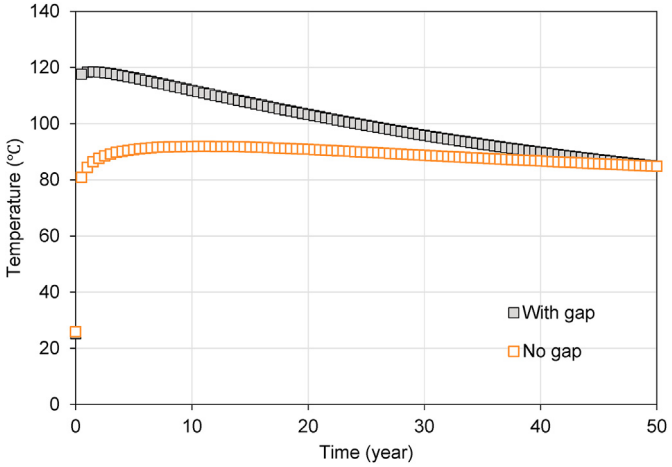

Fig. 4. Temperature variation of buffer materials with and without a gap.

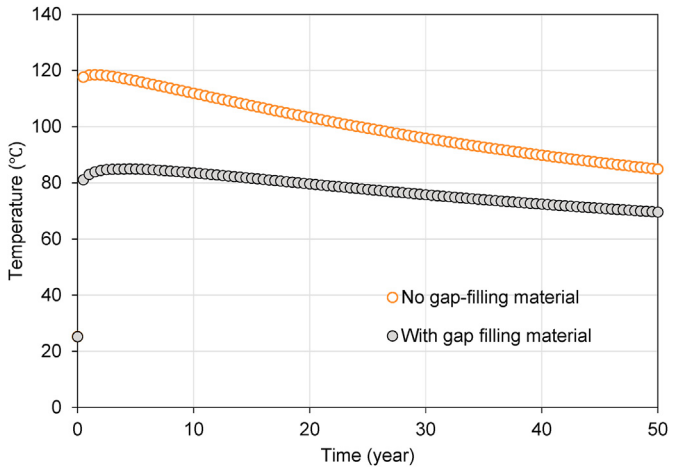

Fig. 5. Temperature variation of buffer materials with and without GFMs.

Table 6
Dimension of EBS components and buffer properties considering a GFM.

Parameters	Description
Specific gravity of block	2.71
Deposition depth (m)	7.78
Diameter of hole (m)	1.75
Bentonite diameter (m)	1.65
Block pile height (m)	7.78
Bentonite volume (m^3)	12.58
Canister volume (m^3)	3.98
Deposition hole volume (m^3)	18.71
Gap volume (m^3)	2.16
Bulk density of bentonite blocks at emplacement (kg/m^3)	2034
Total dry bentonite weight (kg)	22635.02
1) When the outer gap is empty	
Dry density of buffer (kg/m^3)	1536.63
Saturated water content of buffer (%)	28.18
Saturated density of the buffer (kg/m^3)	1969.61
Time to fill gap volume with flow of 0.01 L/min (days)	149.67
Need to swell (%)	17.14
2) When filling the outer gap	
Dry density of buffer (kg/m^3)	1594.51
Saturated water content of buffer (%)	25.81
Saturated density of the buffer (kg/m^3)	2006.13
Time to fill gap volume with flow of 0.01 L/min (days)	87.23
Need to swell (%)	9.99

to 10 mm by applying the Finnish disposal system standard, and the space between the buffer material and the rock was set to 50 mm. As shown in Fig. 4, when a gap exists containing only air, the peak temperature of the buffer material is derived to be approximately 26% higher than it is when there is no gap. Thus, the existence of the gap has a significant effect on the safety evaluation of the disposal system. Therefore, the temperature change of the buffer material was investigated when the outer gap was filled with GFMs, such as granular bentonites, through this study. Fig. 5 shows the temperature change of the buffer material with and without GFMs in the outer gap, and the maximum temperature of the buffer material with a GFM was derived to be approximately 39% lower than that when there was no GFM. This is thought to be because the thermal conductivity of the GFM was approximately 6–7 times higher than that of air. As shown, the GFM must be installed in the outer gap.

4.2. GFM design scheme

In this section, a design plan for a GFM that reflects the KRS$^+$ [34] based on the use of the physical properties of granular bentonite derived above is suggested. As the KRS$^+$ does not reflect the gap space and gap filler, as shown in Table 6, in this study, a design proposal for the GFM such as the gap filling time is presented to calculate the gap filling time according to the dry density, water content, and groundwater inflow rate of the buffer material in the presence and absence of a GFM. Depending on the characteristics of the GFM, the target dry density of the buffer material may vary. Table 7 lists the characteristics of a GFM applied to the design. In particular, when granular bentonite is selected as the GFM, it may be necessary to fill only a small part of the gap with a much smaller amount than that originally required for the entire gap, considering the high-swelling property of granular bentonite. When the KRS$^+$ was applied, the volume occupied by the GFM particles was 0.69 m^3, the volume per mass was ~0.37 ml/g, and the space in which the GFM particles can swell in the gap space was calculated to be equal to 1.18 m^3. The swelling index of the GFM was derived to be ~20 ml/2 g, which is ~27 times the volume per gram the particles occupy in the current gap. Therefore, considering the swelling property of the GFM, if the GFM is installed such that 1/27 of the original amount at the time of initial construction is used, the attained state will be similar to that without the GFM, and the temperature of the buffer material will increase excessively. By simplifying this, Fig. 6 shows the temperature change of the buffer material when the gap is filled with GFM at the ratios of 1/3, 2/3, and 3/3. It can be observed that the maximum temperature of the buffer material was derived to be more than ~29% higher even

Table 7
Required properties of a GFM in the design of EBS components.

GFM and outer gap characteristics	Description
Total density (kg/m^3)	1000
Water content (%)	11
Specific gravity	2.7
Dry density of GFM (kg/m^3)	900.90
Total volume of outer gap, V_t (m^3)	2.08
Weight of GFM particles, W_s (kg)	1871.65
Volume of GFM particles,V_s (m^3)	0.69
Volume of water in GFM, V_w (m^3)	0.21
Volume of air in outer gap, V_a (m^3)	1.18

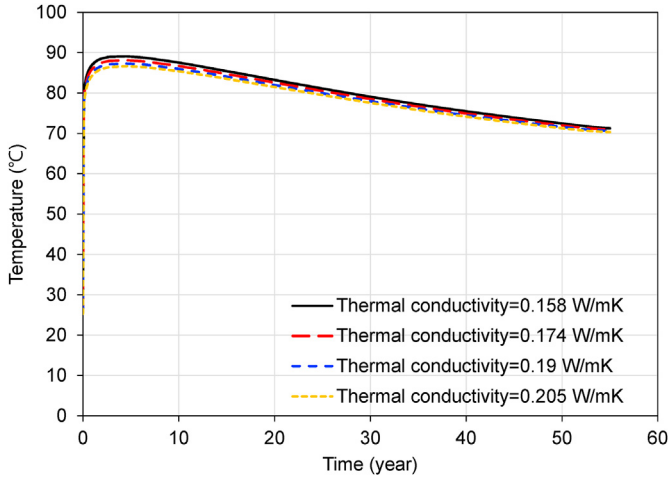

Fig. 7. Temperature variation of buffer materials according to the GFM thermal conductivity.

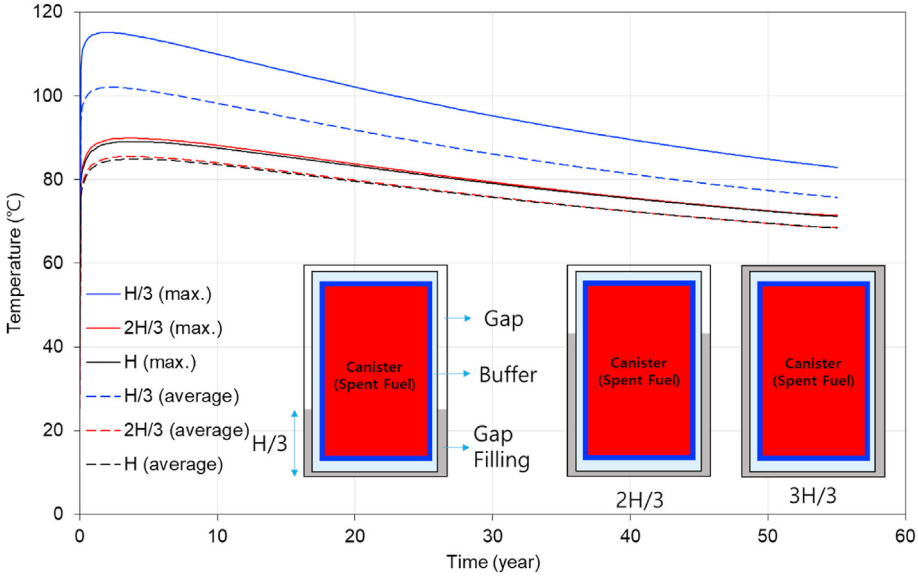

Fig. 6. Temperature variation of buffer materials according to the GFM quantity.

when only 1/3 of the gap was filled with the GFM. Given that the maximum temperature of the buffer material appeared to be approximately 5–20 years after the disposal process, groundwater inflow into the gap between the buffer material and the rock must occur immediately (within 10 years) to meet the reference temperature of the buffer material. If accurate prediction is possible, it will become possible to identify an economical design that can save on the amount of GFM, but the dry density of the buffer material when the gap is almost empty will decrease considerably compared with the initial buffer material block. Thus, there is a disadvantage associated with the matching of the target dry density in that it will be necessary to manufacture a buffer material block with a large dry density value from the beginning. Therefore, it is appropriate to install a GFM with a high initial thermal conductivity, considering the gap, to remove the uncertainty caused by the GFM and ensure a safe design. Fig. 7 shows the change in the temperature of the buffer material according to the initial thermal conductivity of the GFM. It can also be observed that if the thermal conductivity of granular bentonite applied in this study is improved by $\geq$ 20%, the peak temperature of the buffer material is lowered by ~2–3 °C. Therefore, when GFMs are installed, the thermal conductivity of the GFM can be increased if its wet density is increased through compaction and a GFM with high initial water content is used.

5. Conclusions

In this study, the basic characteristics and thermal properties of GFMs, which are located between the components of an engineered barrier system for disposal of HLWs, were investigated. The effect of the gap and GFM on the peak temperature of the buffer material was numerically analyzed. The following conclusions were obtained by presenting the basic design of the GFM to which the KRS^+ was applied.

- Through the numerical analysis considering heat conduction and convection of the air in the gap based on the KRS^+, the peak temperature of the buffer material was derived in the presence and absence of a gap. In particular, the maximum temperature of the buffer material when the gap existed as air was measured to be ~26% higher than that not considering the gap. Thus, it can be observed that the gap has significant effect on the maximum temperature of the buffer material. In addition, when the gap between the buffer material and the rock was filled with GFMs, the maximum temperature of the buffer material was derived to be ~39% lower than when it was not filled. Based on this, it can be shown that the GFM with high initial thermal conductivity must be filled in the space between the buffer material and the rock.
- Considering the KRS^+, it can be shown that the target dry density of the buffer material varied according to the initial moist density, specific gravity, and water content of the GFM. Considering the swelling characteristics of the GFM, the required amount of a GFM can be reduced. However, because it is difficult to predict accurately the time for groundwater inflow and that for the buffer material needed to reach the maximum temperature after the deposition holes are closed, it becomes necessary to fill the entire gap with GFMs. In the future, for more accurate and safer disposal of HLWs, a more accurate GFM design method should be suggested through thermo-hydraulic-mechanical analysis depending on the presence of GFMs.

Declaration of competing interest

The authors declare that they have no known competing financial interests or personal relationships that could have appeared to influence the work reported in this paper.

Acknowledgements

This research was funded by the Basic Research Project (2020R1F1A1072379) and Nuclear Research and Development Program (2021M2E3A2041351) by the National Research Foundation of Korea.

References

[1] W.Z. Chen, Y.S. Ma, H.D. Yu, F.F. Li, X.L. Li, X. Sillen, Effects of temperature and thermally-induced microstructure change on hydraulic conductivity of Boom clay, J. Rock Mech. Geotech. Eng. 9 (2017) 383–395.
[2] L. Zheng, J. Rutqvist, J.T. Birkholzer, H.H. Liu, On the impact of temperature up to 200 °C in clay repositories with bentonite engineered barrier system: a study with coupled thermal, hydrological, chemical, and mechanical modeling, Eng. Geol. 197 (2015) 278–295.
[3] S. Yoon, G.Y. Kim, Measuring thermal conductivity and water suction for variably saturated bentonite, Nucl. Eng. Technol. 53 (2021) 1041–1048.
[4] M. Juvankoski, Buffer Design 2012, Posiva 2012-14, Posiva Oy.
[5] M.J. Kim, S.R. Lee, S. Yoon, J.S. Jeon, M.S. Kim, Effect of thermal properties of bentonite buffer on temperature variation, J. Korean Geotechn. Soc. 34 (1) (2018) 17–24.
[6] M.V. Villar, P.L. Martin, J.M. Barcala, Modification of physical, mechanical and hydraulic properties of bentonite by thermo-hydraulic gradients, Eng. Geol. 81 (2006) 284–297.
[7] D.A. Dixon, M.N. Gray, A.W. Thomas, A study of the compaction properties of potential clay-sand buffer mixtures for use in nuclear fuel waste disposal, Eng. Geol. 21 (1985) 247–255.
[8] O. Karnland, Chemical and Mineralogical Characterization of the Bentonite Buffer for the Acceptance Control Procedure in a KBS-3 Repository, Svensk Kärn-bränslehantering AB Report, 2010. SKB TR-10-60.
[9] A. Lloret, M.V. Villar, M. Sanchez, A. Gens, X. Pintado, E.E. Alonso, Mechanical behavior of heavily compacted bentonite under high suction changes, Geotechnique 53 (2003) 27–40.
[10] G. Xiang, W. Ye, Y. Xu, F.E. Jalal, Swelling deformation of Na-bentonite in solutions containing different cations, Eng. Geol. 277 (2020), 105757.
[11] J.O. Lee, H. Choi, J.Y. Lee, Thermal conductivity of compacted bentonite as a buffer material for a high-level radioactive waste repository, Ann. Nucl. Energy 94 (2016) 848–855.
[12] W.J. Cho, J.O. Lee, S. Kwon, An empirical model for the thermal conductivity of compacted bentonite and a bentonite–sand mixture, Heat Mass Tran. 47 (11) (2011) 1385–1393.
[13] W.J. Cho, J.O. Lee, K.S. Chun, The temperature effects on hydraulic conductivity of compacted bentonite, Appl. Clay Sci. 14 (1999) 47–58.
[14] J.O. Lee, K. Brich, H.J. Choi, Coupled hydro analysis of unsaturated buffer and backfill in a high-level waste repository, Ann. Nucl. Energy 72 (2014) 63–75.
[15] J. Lee, I. Kim, H. Choi, D. Cho, An improved concept of deep geological disposal system considering arising characteristics of spent fuels from domestic nuclear power plants, J. Nucl. Fuel Cycle Waste Technol. 17 (4) (2019) 405–418.
[16] M. Yoo, H.J. Choi, M.S. Lee, S.Y. Lee, Measurement of properties of domestic bentonite for a buffer of an HLW repository, J. Korean Radioact. Waste Soc. 14 (2) (2016) 135–147.
[17] J.O. Lee, Y.C. Choi, H.J. Choi, R&D Status on Gap-Filling Materials for the Buffer and Backfill of a HLW Repository, KAERI/AR-1005/2013, 2013.
[18] P. Marjavaara, H. Kivikoski, Filling the Gap between Buffer and Rock in the Deposition Hole, Working Report 2011-33, Posiva Oy, Eurajoki, 2011.
[19] B. Kjartanson, D. Dixon, C. Kohle, Placement of Bentonite Pellets to Fill Repository Sealing System Voids and Gaps, Technical Report No. 06819-REP-01200-10136-R00, Ontario Power Generation, 2005.
[20] J.O. Lee, H.J. Choi, G.Y. Kim, D.K. Cho, Numerical analysis of the effect of gap-filling options on the maximum peak temperature of a buffer in a HLW repository, Prog. Nucl. Energy 111 (2019) 138–149.
[21] Y.S. Xu, X.Y. Zhou, D.A. Sun, Z.T. Zeng, Thermal properties of GMZ bentonite pellet mixtures subjected to different temperatures for high-level radioactive waste repository, Acta Geotech. 17 (3) (2022) 981–992.
[22] G.J. Lee, S. Yoon, W.J. Cho, Effect of bentonite type on thermal conductivity in a HLW repository, J. Nucl. Fuel Cycle Waste Technol. 19 (3) (2021) 331–338.
[23] W.J. Cho, Bentonite Barrier Material for Radioactive Waste Disposal, KAERI/GP-5352-2-2019, 2019.
[24] I. Bisutii, I. Hilke, M. Raessler, Determination of total organic carbon – an overview of current methods, Trends Anal. Chem. 23 (10–11) (2004) 716–726.
[25] J. Nieuwenhuize, Y.E.M. Maas, J.J. Middelburg, Rapid analysis of organic carbon and nitrogen in particulate materials, Mar. Chem. 45 (1994) 217–224.
[26] H. Park, Thermal Conductivities of Unsaturated Korean Weathered Granite Soils, Master Thesis, KAIST, 2011.
[27] ASTM D5334-14, Standard Test Method for Determination of Thermal Conductivity of Soil and Soft Rock by Thermal Needle Probe Procedure, ASTM International.
[28] K.L. Bristow, R.D. White, G.J. Klutenberg, Comparison of single and dual probes for measuring soil thermal properties with transient heating, Aust. J. Soil Res. 32 (2011) 447–467.

[29] COMSOL Inc, COMSOL Multiphysics User's Manual Version COMSOL 5.5, 2019. City, Sate, USA.
[30] M.J. Kim, S.R. Lee, J.S. Jeon, S. Yoon, Sensitivity analysis of bentonite buffer peak temperature in a high-level waste repository, Ann. Nucl. Energy 123 (2019) 190–199.
[31] F.P. Incropera, D.P. DeWitt, T.L. Bergman, A.S. Lavine, Fundamentals of Heat and Mass Transfer, sixth ed., John Wiley & Sons, City, Country, 2006.
[32] X.Y. Zhou, L.W. He, D.A. Sun, Three-dimensional thermal modeling and dimensioning design in the nuclear waste repository, Int. J. Numer. Anal. Methods GeoMech. 46 (4) (2022) 779–797.
[33] M.J. Kim, G.J. Lee, S. Yoon, Numerical study on the effect of enhanced buffer materials in a high-level radioactive waste repository, Appl. Sci. 11 (18) (2021) 8733.
[34] J. Lee, I. Kim, H. Ju, H. Choi, D. Cho, Proposal of an improved concept design for the deep geological disposal system of spent nuclear fuel in Korea, J. Nuclr. Fuel Cycle and Waste Technol. (JNFCWT) 18 (spc) (2020) 1–19.